HHS Public Access

Author manuscript

Nat Biotechnol. Author manuscript; available in PMC 2020 December 29.

Published in final edited form as:

Nat Biotechnol. 2020 November ; 38(11): 1280–1287. doi:10.1038/s41587-020-0547-7.

A tissue-engineered uterus supports live births in rabbits

Renata S. Magalhaes, **J. Koudy Williams**, **Kyung W. Yoo**, **James J. Yoo**, **Anthony Atala***

Wake Forest Institute for Regenerative Medicine, Wake Forest University, School of Medicine, Medical Center Boulevard, Winston-Salem, North Carolina, USA.

Abstract

Bioengineered uterine tissue could provide a treatment option for women with uterine factor infertility. In large-animal models, reconstruction of the uterus has been demonstrated only with xenogeneic tissue grafts. Here we use biodegradable polymer scaffolds seeded with autologous cells to restore uterine structure and function in rabbits. Rabbits underwent a subtotal uterine excision and were reconstructed either with autologous cell-seeded constructs, with non-seeded scaffolds, or by suturing. At 6 months post-implantation, only the cell-seeded engineered uteri developed native tissue-like structures, including organized luminal/glandular epithelium, stroma, vascularized mucosa, and two-layered myometrium. Only rabbits with cell-seeded constructs had normal pregnancies (4/10) within the reconstructed segment of the uterus and supported fetal development to term and live birth. With further development, this approach may provide a regenerative medicine solution to uterine factor infertility.

The uterus supports many complex biological functions that are essential for mammalian reproduction[1]. Factors adversely affecting uterine integrity, such as congenital anomalies or acquired diseases, may compromise a woman's ability to conceive or to carry a viable fetus to term[2,3]. Approximately 6% of women undergoing infertility treatments have a dysfunctional uterus[4]. Allogeneic uterine transplantation has shown promise as a treatment for permanent uterine infertility[5–7], although it requires donors and the use of anti-rejection therapies. Since 2014, live births have been reported in women who received transplanted uteri[8,9]. Regenerative medicine and tissue engineering technologies have emerged as an attractive option for overcoming donor organ shortages and other limitations of allogeneic

***Corresponding Author:** Anthony Atala, aatala@wakehealth.edu.

Author contributions

A.A. developed the concept of engineering functional autologous uterine tissue constructs. R.S.M., J.K.W., J.J.Y., and AA designed all experiments. R.S.M. performed the in vitro experiments and fabricated the bioengineered uterine constructs. R.S.M. and J.K.W. performed in vivo experiments of uterine tissue excision and construct implantation. K.W.Y. performed in vitro experiments and analyzed the data. R.S.M., J.K.W., and A.A. analyzed the data and wrote the manuscript. A.A. provided direction and supervised the project. R.S.M., J.K.W., J.J.Y., and A.A. reviewed and edited the manuscript.

Competing interests

Boston Children's Hospital was assigned the rights to two issued patents, both titled "Tissue Engineered Uterus", #7,049,057, filed November 15, 2002, and #7,429,490, filed February 7, 2005, with Anthony Atala and James J. Yoo listed as inventors. Based on the remaining patent term and the need for further studies before this technology is used clinically, there are no current or expected financial interests related to these patents.

Life Sciences Reporting Summary Further information on research design is available in the Nature Research Reporting Summary linked to this article.

transplantation[10]. Creating tissue and organ substitutes from a patient's own cells combined with biomaterials minimizes the risks of immunological rejection and disease transmission. This approach has enabled the implantation of bioengineered bladders[11], blood vessels[12,13], urethras[14], and vaginas[15] in human patients.

Previous work on regeneration of the uterus has proved successful only for small defects that do not have the critical size needed for clinical translation. In rodent models, small uterine defects regenerated when repaired with a variety of biomaterials alone, without the use of cells, such as non-degradable synthetic polymer scaffolds, biodegradable synthetic polymer scaffolds, naturally derived scaffolds, and even scar tissue[16,17]. However, attempts at regenerating larger uterine defects using these strategies have failed. Moreover, rodent organs, including the uterus, have an inherent regenerative capacity. Thus, results obtained in rodent models may not translate to larger animal models and humans. Only two published studies have explored uterine regeneration in an animal model larger than rats. One study used human umbilical vein grafts as a segmental graft in rabbits and reported grafts with epithelial layer reorganization but minimal myometrial tissue ingrowth[18]. In the second study, porcine small-intestinal submucosa acellular grafts ranging from 0.5 to 2 cm in length by 0.7 – 0.8 cm were engrafted in rabbits, and the success of the study was limited as the graft size increased[19]. It was noted that grafts 1 cm or longer collapsed, resulting in total architectural disruption.

Findings in other rabbit studies on reconstruction of hollow structures, such as tubular urethras, also demonstrated abnormal regeneration when using 1 cm acellular matrices alone, but if cells were seeded on the same 1 cm matrices, normal regeneration would occur[20]. Acellular matrices covering defect areas allow cells from the normal native tissue edge to move across the matrix, creating new tissue. The maximum defect distance suitable for normal urethral tissue formation in rabbits using acellular grafts that rely on the surrounding native tissue cells for regeneration is 0.5 cm[21]. If the biomaterial distance is greater than 0.5 cm from any native edge, there is still some cell migration from the native tissue, but fibroblast deposition takes over, leading to scar formation. This also explains, in part, why rodent animal models are not ideal for regeneration studies, as the size of the defects created in most instances may not be clinically meaningful, and why prior rabbit studies with larger defects failed. Because of the inherent regenerative capacity of small segments of tissue in rodent models, larger animal models, where one can replace critical-size defects with engineered constructs, are important in highlighting potentially human clinically-relevant regeneration, both scientifically, and for advancing these technologies to humans. Rabbits have long been used in reproductive biology research and are ideal for uterine tissue regeneration studies as they have a relatively large uterus compared with other laboratory animals, with two separated functional uterine horns and cervices, each with a capacity to carry a pregnancy[22].

Our strategy to bioengineer functional tissues using autologous primary cells seeded onto biodegradable scaffolds has been effectively explored in pre-clinical studies[20,23–26], and applied successfully in human patients to restore function in tubular organs such as the urethra[14], and in hollow non-tubular organs, such as the bladder[11] and vagina[15]. We now follow the same approach to engineer the uterus, a more complex organ with higher

functional requirements involving support of embryo implantation and fetal development. We describe the in vitro fabrication of engineered uterine tissue and its development in a rabbit model of subtotal uterine reconstruction. We used biodegradable polymer scaffolds, 6 to 8 cm in length and 2.5 cm in width, composed of poly-DL-lactide-co-glycolide (PLGA)-coated polyglycolic acid (PGA) seeded with primary uterine-derived cells. We have previously used PGA in human patients combined with PLGA to engineer urethras[14], and combined with collagen to engineer bladders[11]. PGA and PLGA polymer biomaterials have been used in tissue engineering due to their unique properties, including high porosity and interconnectivity between pores, high surface-to-volume ratio, versatility of chemistry, tunable mechanical properties, and biocompatibility[27] .

We describe the in vitro fabrication of engineered uterine tissue and its development in a rabbit model of subtotal uterine reconstruction. Over time, the engineered uterine tissue formed patent cavities, organized cellular and anatomical structures within the

endometrium and myometrium compartments. Our reproductive studies showed that autologous tissue engineered constructs supported late-stage pregnancies and viable live births.

RESULTS

Rabbits underwent full excision of one uterine horn and a subtotal excision of the remaining uterine horn, and were divided into three experimental groups, with two groups receiving either a tissue engineered scaffold or a non-seeded scaffold, and a third group where the remaining uterine edges were sutured together. Rabbits from all three experimental groups tolerated the procedures well and subsequently underwent reproductive studies and tissue analyses (Supplementary Fig.1)

Characterization of cultured primary uterine cell.

Cells used for seeding the scaffolds were collected from a full thickness biopsy of the excised uterine horn. Cells were characterized using immunocytochemistry and flow cytometry. The inner layer of the full thickness uterine biopsies (Supplementary Fig.2a) yielded cuboidal and elongated cells (Supplementary Fig.2b) that expressed epithelial and stromal markers cytokeratin AE1/AE3 (1:50, ab28028; Abcam; Supplementary Fig.2c) and vimentin (1:100, ab28028; Abcam; Supplementary Fig. 2d), respectively. The outer layer of the uterine biopsies yielded spindle shaped smooth muscle-like cells (Supplementary Fig.2e) that were positive for smooth muscle myosin heavy chain 11 (MHC, 1:250 ab683; Abcam), calponin (1:100, C2687; Sigma-Aldrich), and smooth muscle alpha-actin (α-SMA, 1:40, ab18147; Abcam; Supplementary Fig. 2 f–h). Flow cytometric analyses of third-passage cultured cells showed that a high percentage of the endometrium-derived samples expressed the epithelial cell marker CD9[28,29] (1:100, CBL162P; Millipore; 78%) and stromal marker vimentin (1:100; 96%), while myometrium-derived cultures expressed αSMA (1:100; 96%) and calponin (1:100; 90%) (Supplementary Figs. 2 i–l; and Supplementary Fig. 2 m for flow cytometry gating). These phenotypes and cell marker profiles are consistent with native endometrial and myometrial cells and aligned with previous reports that primary uterine cells, without fibroblast overgrowth, are stable in culture systems for over 10 passages[30].

Fabrication of the uterine constructs.

PGA/PLGA scaffolds were tailor-made in semi-circular shapes (Fig 1a). Scanning electron microscopy (SEM) micrographs of representative samples of the synthetic polymer scaffolds depicted a 3-D interconnected porous network (Fig. 1b). Ten million cells/cm^2 collected from the myometrium-derived cultures were seeded on the outer layer of the scaffold and ten million endometrium-derived cells/cm^2 were successfully seeded on the inside of the scaffold using a sequential seeding method. SEM analysis of the PGA/PLGA seeded scaffolds showed uniform cell attachment throughout the length and thickness of constructs during the in vitro incubation period (Fig. 1c).

Implantation of the uterine constructs.

At the time of the experimental implantation procedure, the rabbits had a subtotal semi-circular excision of their remaining uterine horn and received either a cell-seeded construct, a non-seeded scaffold, or had the defect repaired by suturing the remaining edges. Titanium clips were used to delineate the margin between the native tissue and the area of scaffold implantation. An additional normal control group underwent a sham laparotomy. The surgical procedures (Fig. 1e–f) were uneventful and no major postoperative complications were observed during the study.

In vivo analyses of uterine constructs.

Thirty-six of the 78 animals were sacrificed at 1, 3, or 6 months after the experimental uterine surgeries for analyses (n=3 per experimental group per time point). During necropsy, the reproductive tract was inspected for gross abnormalities. The uterine surgical sites were identified in all experimental animals. Specimens were retrieved from the engrafted area, identified by the presence of marking sutures and titanium clips, and then submitted for histological analysis.

Gross findings.

Gross macroscopic observations at 1 month after surgery showed mild adhesions between the uterus and adjacent organs (bladder and intestine), as well as a partially degraded biomaterial in the scaffold groups. Animals in the subtotal excision-only group had anastomotic strictures and hydrometra in 67% of the retrieved uterine horns. At 3 and 6 months, the polymer scaffold material was not visually present in the engineered uteri group or in the non-seeded scaffold group. At 6 months, the subtotal excision-only group had areas of exposed endometrium and fibrotic scars along the surgical site. Prior to euthanasia contrast medium was instilled into the cervical canal under fluoroscopic observation to investigate the morphology of the uterine cavities. Serial hysterograms taken at 6 months showed that the tissue engineered group had patent cavities with a preserved uterine configuration (Supplementary Fig. 3a). The non-seeded scaffold group had multiple filling defects and marked strictures along the lumen of the implanted uterine horn (Supplementary Fig. 3b). The subtotal excision-only controls had severe proximal luminal blockage with incomplete contrast filling of the cavity (Supplementary Fig. 3c). The normal control uterine horns showed patent cavities that resembled the tissue engineered uteri group (Supplementary Fig. 3d).

Immuno-histological/molecular findings.

Tissue cross-sections were stained with Masson's trichrome and used to calculate the relative collagen and smooth muscle content in samples retrieved at 1, 3, and 6 months. At 1 month post implantation, we observed that the scaffold material had partially degraded histologically and maintained the luminal cavity structure in animals receiving tissue engineered uterine constructs and non-seeded scaffolds (Fig. 2a, b). In contrast, the subtotal excision-only controls showed abundant granulomatous tissue formation and complete luminal stenosis (Fig. 2c). At the anastomosis site, we observed initial tissue growth in all experimental groups, but the tissue engineered uteri group had greater full-thickness cellular coverage surrounding the polymer fibers (Fig. 2 a middle-bottom) with less collagen content than non-seeded scaffold group and subtotal excision-only controls (37± 5%, 68 ± 4%, 64 ± 4%, respectively; $p < 0.01$) (Fig. 2m). Three months post-surgery, the scaffold material underwent complete biodegradation. The tissue engineered uteri group had developed an epithelial lining, distinct stroma with glandular structures (Fig. 2e middle), and smooth muscle bundles in the outer layer (Fig 2e bottom). The non-seeded scaffold group had epithelial coverage, partially formed stromal layer (Fig. 2f middle), scarce smooth muscle fibers (Fig. 2f bottom), and greater collagen content compared to the tissue engineered group (61± 5% vs. 39 ± 3%; $p < 0.01$) and normal controls (61± 5% vs. 25 ± 2%; $p < 0.001$) (Fig. 2m). The subtotal excision-only controls had an incomplete development of the endometrial and myometrial layers (Fig. 2g) and greater collagen content than normal controls (53 ± 3% vs. 25 ± 2%; $p < 0.01$) (Fig 2m).

At 6 months post-implantation, there were no obvious histologic boundaries between the native uterine tissue edges and the tissue engineered constructs (Fig. 2i). The tissue engineered uteri group formed inner circular and outer longitudinal layers (Fig. 2i bottom) of smooth muscle bundles, with less collagen content than the non-seeded scaffold group (47 ± 1% vs. 66 ± 6%; $p < 0.05$), and higher than the normal controls (47 ± 1% vs. 25 ± 2%; $p < 0.05$) (Fig. 2m). The relative expression of αSMA by Western blot analyses in the tissue engineered group (0.8 ± 0.5) and subtotal-excision group (1 ± 0.2) was similar to normal controls (1.2 ± 0.1; $p = 0.16$) and significantly lower in the non-seeded group (0.4 ± 0.2; $p < 0.01$) (Supplementary Figs. 4 a, b; and 5 for full Western blot gel image). The two-layered distribution of smooth muscle bundles in the neo-uterine tissue was confirmed using immunostaining for αSMA (Supplementary Fig. 4c).

We also evaluated the neo-uterine mucosa, including endometrium thickness, vascularization, and gland density. H&E cross-sections were used to measure endometrium thickness and gland density per field. CD31 immunostaining was used to assess blood vessel endothelium. Among experimental groups, only the tissue engineered uteri group formed native-like epithelial crypts (Fig.3a). In addition, the tissue engineered uteri group had endometrial gland and blood vessel densities comparable to normal controls ($p = 0.98$; $p = 0.95$, respectively) (Fig. 3b, j, k); and greater endometrium thickness than non-seeded scaffold group and subtotal excision-only controls (315.6 ± 129.5 μm, 166.6 ± 48.1μm, 167.1 ± 65.3 μm, respectively; $p<0.01$) (Fig. 3i).

To further assess the in vivo maturation of the tissue engineered uteri, we confirmed the expression of hormone receptors such as estrogen receptor alpha (Fig. 4a) and progesterone

receptor (Fig. 4b), as well as the secretory protein uteroglobin (Fig. 4c), which is located in uterine epithelial cells and is associated with rabbit reproductive function.

Collectively, these results indicate that the tissue engineered uteri group formed patent lumina with vascularized native uterine tissue-like structures. In contrast, the non-seeded scaffold group had a sparse cellular structure and lumen-occlusive scar formation. Histological features found in the subtotal excision-only controls showed a poorly formed uterine structure, consisting primarily of scar tissue.

Pregnancy outcomes.

To investigate the in vivo functionality of the engineered uterine tissue, we conducted reproductive studies using fertile males for natural mating starting 6 months after uterine reconstruction procedures. Pregnancy studies were done in 42 of the 78 rabbits. Animals were assigned to four groups: the tissue engineered uteri group (n=14), non-seeded scaffold group (n=14), subtotal uterine excision-only controls (n=7), and normal controls (n=7). The reproductive outcomes are depicted in Table 1. Pregnancies were identified 29–30 days post-successful mating (identifying sperm within the vagina following mating) by visualizing fetal bone formation with standard x-rays. Location of the fetuses within the uterus was investigated via computed tomography (CT) by identifying fetus location relative to the titanium clips-demarcated segment (Fig. 5a), which was then confirmed macroscopically during surgical delivery (Fig. 5b–c). Only the rabbits receiving the tissue engineered constructs had normal pregnancies within the reconstructed segment of the uterus (4/10 rabbits). There were no congenital malformations found at necropsy (Fig. 5d), and the average delivered fetus body weights were comparable to normal controls ($p = 0.994$), suggesting that the engineered uteri supported normal fetal development. Viable pregnancies also occurred within the remaining cervical end native uterine tissue, proximal to the reconstructed segments. The non-seeded scaffold constructs and subtotal excision-only controls had no fetal development or placentation. While placentation occurred around the circumference of the bioengineered construct segment, it was not possible to demarcate the exact line of distinction between the engineered tissue and native tissue (Fig. 5e). There was no macroscopic evidence of defects or herniation along the pregnant engineered uterus, and histological analyses confirmed normal uterine tissue structures (Fig. 5 f–g) and placental development (Fig. h-k). The results indicate that the tissue engineered uteri achieved reproductive function, and responded to the expansion and mechanical strains that occur during pregnancy, allowing appropriate growth and intra-utero survival of the fetuses until late stages, supporting live births.

DISCUSSION

We report a regenerative medicine-based approach to create functional neo-uterine tissues that support pregnancy to term and live births in a large animal model. Our results demonstrate that an autologous cell-seeded bioengineered uterine construct develops all uterine tissue layers, including a vascularized endometrium with secretory gland structures and 2-layered myometrium, within six months after implantation in a subtotally excised rabbit uterine horn. We also show that intrinsic regenerative mechanisms alone do not

support functional restoration of uterine tissue layers following a large excision. The fundamental role of the uterus is to allow embryo implantation, fetal nourishment, and growth. The advantages of using rabbits for reproductive studies include: 1) females are always in estrus and ovulation is induced by mating, resulting in an exactly defined pregnancy stage, 2) they have a short reproductive cycle (pregnancy lasts for 31 days), and 3) placental morphology and function are similar to humans[22].

In the present study, six months post engraftment, only the tissue engineered uteri group supported pregnancy and normal fetal development to term within the length of the reconstructed segment after natural mating, resulting in well-formed offspring with body weights similar to normal rabbits. Unlike rodents, leporine early embryo development differs and is more relevant, as the first contact with a receptive endometrium occurs in the anti-mesometrial side at the time of blastocyst attachment, and a displacement over the mesometrial side subsequently occurs where the placenta eventually develops[31]. All experimental animals had the anti-mesometrial side removed, but only the uteri with the construct seeded with cells, the bioengineered uteri group, achieved successful blastocyst-endometrium interactions that resulted in normal placentation in the mesometrial side and normal fetal development. CT imaging and macroscopic findings at delivery confirmed placentation along the mesometrial region of the tissue engineered segment. Notably, it was not possible to demarcate the exact line between the bioengineered construct and the retained mesometrium, because the pregnant engineered tissue was indistinguishable from the native tissue. The bioengineered construct supported stretch-induced tissue expansion (more than ten times its weight) and remodeling that occurs during pregnancy to accommodate the growing fetus, placenta, and amniotic fluid, and supported formation of viable offspring with body weights similar to those of the normal controls, which suggests normal placental function. Although the number of fetuses per pregnancy was lower than in the normal controls, the overall reproductive function of the tissue-engineered uteri was re-established, allowing fetal development and pregnancies to term with live births in 4 out of 14 cases. The lack of reproductive outcomes observed in the non-seeded scaffolds and subtotal excision-only uteri are likely due to the multiple luminal strictures and incomplete development of all the tissue structures, including endometrial glands, that were noted in the study.

Small uterine defects are able to regenerate intrinsically. The regenerative capacity of small uterine defects has been shown with various synthetic biomaterials, including biodegradable polyetherurethane/poly-L-lactide or nonbiodegradable polytetrafluoroethylene[32]. Both scaffold grafts, without any added cells, led to endometrial regeneration in rodents. Naturally-derived materials without cells have also been used as scaffolds for partial uterine reconstruction in rodents, including decellularized uterine tissue and boiled blood clot derived avascular scar tissue composed of myofibroblasts and collagen[33,34]. Commercially available bovine derived freeze-dried collagen extract membranes, either with growth factors (bFGF), with cells derived from human embryonic stem cells, or with bone marrow derived stem cells, have been used for the replacement of uterine horn segments[35–37]. Other studies using decellularized segments of uterine mucosa seeded with either rat uterine primary cells alone[38] or together with commercially purchased rat MSCs[39] also showed successful regeneration. In all the rodent studies described, when small uterine defects were created,

and repairs were attempted either with or without the use of naturally-derived scaffolds, and either with or without the use of cells or growth factors, uterine regeneration with subsequent pregnancies were reported. Porcine small-intestinal submucosa grafts without the use of cells were also investigated for uterine reconstruction in rabbits[19]. Similar to the rodent studies, the smaller grafts, less or equal to 1 cm, supported reproductive function, and a common complication of a longer graft was graft collapse or twisting, confirming the inherent regenerative capacity of small uterine tissue segments, and underscoring the challenges encountered when attempting to regenerate larger tissue defects. Tissue engineering strategies to replace critical-size defects and demonstrate clinically-relevant regeneration are needed. In our studies in rabbits, synthetic biodegradable polymer scaffolds, 6 to 8 cm in length and 2.5 cm in width were used to engineer uterine tissue.

Synthetic polymer materials have been widely used as scaffolds for engineering tissues, are Food and Drug Administration-approved for human application, and are suitable for reconstructive surgery in selected patients[11,14]. The advantage of using synthetic polymer scaffolds is that they can be produced on a large scale and controlled for physical properties such as tensile strength, degradation rate, and three-dimensional design.

We demonstrated that rabbit autologous primary uterine cells can be expanded ex vivo efficiently and successfully attach to PGA/PLGA scaffolds for large uterine reconstructive purposes. From an immunologic perspective, autologous cell sources are advantageous for the development of implantable-engineered tissues. The engineered uterine tissue supported pregnancy and normal fetal development to term, resulting in well-formed offspring. Our results introduce new avenues for potentially creating tissue substitutes derived from a patient's own cells to treat uterine defects. Further preclinical studies are being planned before clinical trials are contemplated.

Animal Protocol.

All animal experiments were performed with the approval of the Institutional Animal Care and Use Committee and in accordance with all federal guidelines. Rabbits were euthanized according to the guidelines set forth by the American Veterinary Medicine Association.

Experimental design.

Female New Zealand rabbits (3.5–4 kg) were purchased from Charles River Laboratories (Wilmington, MA) and single-housed at the Wake Forest University animal facility. They were fed standard rabbit chow (Purina, Largo, FL), received water ad libitum, and were kept in rooms with automatically controlled temperature (22.0 +/– 0.1°C) and light-dark cycles (14 hours of light and 10 hours of dark). A total of 78 animals were randomly assigned to four groups: 1) a tissue engineered uteri group (n=23) where the subtotal excision was repaired with an autologous cell-seeded scaffold; 2) a non-seeded scaffold group (n=23), where the subtotal excision was repaired with a polymer scaffold only; 3) a subtotal uterine excision-only control group (n=16), where the subtotal excision was repaired by suturing the remaining edges together; 4) and a normal control group (n=16), where animals underwent a sham laparotomy.

Uterine tissue harvest and cell isolation.

Under general anesthesia (2–5% isoflurane) and using aseptic technique, one uterine horn was identified through a midline laparotomy and completely excised from all rabbits. The uterine horn was transported in cold Dulbecco's phosphate-buffered saline (DPBS; 14190136; ThermoFisher Scientific) supplemented with 1% antibiotic and antimycotic (SV3007901; ThermoFisher Scientific). Using aseptic techniques, the uterine tissue was transferred to a petri dish, dissected free of connective tissue, opened lengthwise, and washed with cold DPBS (14190136; ThermoFisher Scientific) to remove any debris. The endometrial lining was gently scrapped off and minced into 1 mm^3 pieces using a scalpel, and then transferred to a 6-well tissue culture plate (353046; Corning). The myometrium tissue layer was then minced into 1–2 mm^3 pieces and transferred to a different 6-well culture plate (353046; Corning) for smooth muscle cell isolation. Three to four pieces of tissue were disposed per well to allow for optimal cell outgrowth.

After the explants adhered to the dish surface (5 minutes), endometrium culture media containing Dulbecco's Modified Eagle's growth medium (DMEM) - F12 (SH3026101; ThermoFisher Scientific) supplemented with 10% fetal bovine serum (FBS; 100–500; Gemini Bioproducts), epidermal growth factor recombinant human protein (5 ng/mL; PHG0315; ThermoFisher Scientific), bovine pituitary extract (40 ng/mL; 13028014;ThermoFisher Scientific), and 1% antibiotic/antimycotic solution (SV3007901; ThermoFisher Scientific) was gently added to the endometrial samples. In a separate culture dish, myometrium media containing high-glucose DMEM (SH30243FS; ThermoFisher Scientific) supplemented with 10% FBS (100–500; Gemini Bioproducts) and 1% antibiotic/antimycotic solution (SV3007901; ThermoFisher Scientific) was added to myometrial tissue explants. The uterine explants were incubated in humidified chambers at 37°C and 5% CO_2 until cell outgrowth was observed (4–5 days), after which the residual tissue pieces were gently removed using sterile forceps. The initial stage of cell growth was termed passage 0. At day 7–10, cell yield was 3–6 million primary uterine cells for each population. Isolated passage 0 primary cells were plated into 75 cm^2 culture flasks (156472; ThermoFisher Scientific). Primary uterine-derived cells were subcultured every 8–10 days and plated in 175 cm^2 culture flasks (159910; ThermoFisher Scientific), 1000 cm^2 culture flasks (PFHYS1008; Millipore), and 2528 cm^2 (140360; ThermoFisher Scientific) culture flasks from passage 1 through passage 3 respectively, to obtain sufficient cells for seeding a uterine scaffold. Culture media was replaced every 2–3 days and cells were dissociated using trypsin-EDTA (25300120; ThermoFisher Scientific) and subcultured (passaged) every 8–10 days, when cell growth reached 80–90% confluence (% coverage of cells in the culture plate/flask). The final cell yield was 150–300 million cells for each population. The average time elapsed between uterine tissue harvest and engineered uterine construct implantation was 38 ± 5.9 days.

Characterization of isolated endometrium- and myometrium-derived cells.

We performed immunocytochemical and flow cytometric analyses to characterize the primary isolated uterine cell phenotypes. For immunofluorescence staining, cells were cultured on 8-well chamber slides, fixed, permeabilized with 100% ice-cold methanol for 15 minutes, and washed before adding blocking solution (Protein Block Serum-free, X0909;

Dako) for 30 minutes at room temperature (RT). Cells were incubated overnight at 4°C with the following primary antibodies separately: anti-pan cytokeratin (AE1/AE3, 1:50, ab28028; Abcam), vimentin (1:100, ab28028; Abcam), smooth muscle myosin heavy chain 11 (MHC, 1:250 ab683; Abcam), calponin (1:100, C2687; Sigma-Aldrich), and smooth muscle alpha-actin (α-SMA, 1:40, ab18147; Abcam). Samples were washed and incubated for 30 minutes at RT with either goat anti-mouse Alexa Fluor 488 (1:500, A11017; ThermoFisher Scientific) or Alexa Fluor 594 (1:100, A11020; ThermoFisher Scientific) secondary antibodies. Slides were mounted in ProLong® Gold antifade with DAPI (P36931; ThermoFisher Scientific), protected from light, and analyzed with a Leica Upright Fluorescent microscope under a magnification of 400X.

For flow cytometric analysis, 200,000 uterine-derived cells were collected in separate tubes, fixed in 4% formaldehyde for 20 minutes, and treated with a blocking solution containing 0.1% Triton X-100 and 3% bovine serum albumin (A-9647; Sigma-Aldrich) for one hour at RT. Uterine-derived cells were immunolabeled with the following primary antibodies: R-phycoerythrin-conjugated CD9 (1:100, CBL162P; Millipore), vimentin (1:100, ab28028; Abcam), α-SMA (1:100, ab18147; Abcam), or calponin (1:100, C2687; Sigma-Aldrich) for one hour at RT; followed by incubation with fluorescein isothiocyanate (FITC)-conjugated IgG (1:250, ab79092; Abcam) for 60 minutes. Negative controls included phycoerythrin-labeled mouse IgG2b, K Isotype (559529; BD Pharmingen), and FITC mouse IgG2a (ab79092; Abcam). Samples were analyzed using a FACSCalibur instrument (Becton Dickinson Immunocytometry Systems).

Bioengineering autologous uterine tissues.

Two mm-thick non-woven biodegradable polymer membrane composed of polyglycolic acid (PGA; Biomedical Structures, Warwick, RI) with a bulk density of 60 mg/mL, 15 μm fibers, inter-fiber distance of 100–200 μm, and 95% porosity were cut and coated with poly-DL-lactide-co-glycolide (PLGA, 50:50; Sigma-Aldrich) in chloroform (5% w/v). In a fume hood, the PGA membrane was completely immersed in 5% PLGA solution until completely saturated. The PGA-PLGA coated scaffold was allowed to evaporate for 30 minutes and then was configured into a semi-circular shape, suturing the edges (6–0 Vicryl® sutures-Ethicon) around a Pasteur glass pipette (1367820B; ThermoFisher Scientific). A second coating process was performed, submerging the semi-circular scaffold in 5% PLGA solution until complete saturation. The solvent was allowed to evaporate for 2 hours, and the scaffolds were kept in a desiccator for 24–48 hours prior to sterilization with ethylene oxide gas.

Polymer scaffold constructs were custom-made for each animal based on measurements taken at the excised uterine horn. The bioengineered constructs ranged from 6–8 cm in length and 2.5 cm in width. Prior to cell-seeding, the sutures were removed using sterile techniques and scaffolds were pre-wetted with myometrium medium and incubated overnight in humidified chambers at 37°C and 5% CO_2.Third-passage myometrial-derived cells (8×10^7 cells/mL) were seeded onto the outer side of the scaffolds and cultured for 4–5 days in humidified chambers at 37°C and 5% CO_2. The constructs were then turned over using sterile forceps, and passage 3 endometrial-derived cells (8×10^7 cells/mL) were

seeded on the inner surface of the scaffold and incubated for an additional 4–5 days in humidified chambers at 37°C and 5% CO_2. A total of ten million cell/cm^2 of each cell population were seeded into the scaffolds. The stepwise seeding process involved gently pipetting cells onto the scaffold surface in a uniform layer. On the outer side, cell seeding was carried out from the top convex surface outward uniformly along the length of the scaffold; and in the inner surface, cells were seeded from the edges toward the concave surface. Seeded scaffolds were transferred to a 150 mm dish (BP140–02; Corning), placed inside a silicone frame (5827T44; McMaster-Carr) to prevent contact to the bottom of the dish, and incubated for two hours at 37°C to allow for cell attachment before being immersed in culture media. The medium was changed every 24 hours, and constructs were incubated in serum-free media for 24 hours before implantation. Non-seeded scaffolds were prepared for implantation identically to that of the cell-seeded scaffolds except without the addition of cells.

Representative samples of the constructs were subjected to microstructural analyses; these samples were fixed in 2.5% glutaraldehyde, dehydrated in ethanol, and dried overnight. The scaffolds were then sputter coated with gold (Hummer 6.2, Anatech) and imaged with a Hitachi S570 system scanning electron microscopic (SEM) (Hitachi Hi-Tech), with an accelerated voltage of 25 kV and 120X magnification.

Uterine construct implantation.

Under general anesthesia, animals were prepared for aseptic surgery, and a lower midline incision was performed to expose the uterus. A semicircular full-thickness segment of 6–8 cm in length (depending on individual differences in the recipient uterus) was excised from the remaining uterine horn, retaining a native tissue strip of 2–3 mm in the mesometrium side (vascular pedicle) and 0.5–1 cm in length of the nearby native tissue proximally (cervical end) and distally (tubal end) for anastomosis (Figure 1 d–f). Uterine bioengineered constructs were sutured in place using a simple interrupted pattern with 6–0 Vicryl® sutures (Ethicon) to replace the excised segment and restore the uterine horn shape. In the uterine subtotal excision-only group, the residual native uterine tissue was closed using 6–0 Vicryl® sutures with no construct implanted. Non-absorbable tag sutures (6–0 Prolene® suture, Ethicon) as well as small titanium clips (Horizon™; Teleflex) were placed proximally, distally, and longitudinally to the anastomotic sites for future identification of the operated area. Upon completion of the implantation procedure, the uterus was inserted back into the abdomen and the incision was closed.

In the normal control group, rabbits underwent a sham laparotomy wherein the uterine horn was exposed and returned to the abdominal cavity, followed with incision closure. All animals were transferred to their housing units upon anesthetic recovery, where they were administered analgesics and provided appropriate post-operative care.

Uterine morphology and immune-histological analyses.

Thirty-six of the 78 animals were sacrificed at 1, 3, or 6 months after scaffold implantation surgery for morphological and histological analyses (n=3 per experimental group per time point) after scaffold implantation surgery. Prior to euthanasia, hysterograms were performed

under fluoroscopy to assess uterine lumen characteristics. Animals were anesthetized, placed on a fluoroscopy table, and diluted (1:10) contrast medium (Conray®, iothalamate meglumine injection U.S.P. 60%) was instilled into the uterine cavity through the cervical canal via a cannula. Digital fluoroscopic images were acquired using the Siremobil compact L system (Siemens).

Tissue samples from the engrafted area were retrieved for histological assessment. Specimens were fixed in 10% neutral buffered formalin for 48 hours, processed (ASP300S; Leica Biosystems), and paraffin-embedded (EG1160; Leica Biosystems). Serial paraffin cross-sections (7 μm) were prepared and either stained with hematoxylin and eosin (H&E) using an automated stainer (ST5010 autostainer XL; Leica Biosystems) or Masson's Trichrome (MT).

Three slides containing cross-sections from the retrieved tissues (n=3 per experimental group per time-point) were imaged using a motorized inverted microscope (Olympus IX83), and digitized for further morphometric analysis. The endometrial thickness was estimated by measuring the points of greatest perpendicular depth (n=4 per field) at the anti-mesometrial area from the luminal surface to the endometrium-myometrium interface under a magnification of 100×. To determine uterine gland abundance, microscopic fields were randomly selected in the lateral and anti-mesometrial sides of each section using a 20× objective, and the number of uterine gland cross-sections was calculated and normalized per endometrial area.

Images captured from MT stained slides (under a magnification of 100×) were used to determine the relative content of collagen/connective tissue (blue) and smooth muscle (red) in the uterine tissue. The relative collagen content was calculated as the total amount of blue stained areas divided by the sum of all red and blue stained areas in the regions of interest (ROI) in three high-power fields. The uterine lumen and blank areas were subtracted from all calculations for accuracy.

For immunohistochemistry (IHC), sections were blocked with avidin/biotin kit (SP-2001; Vector Laboratories) and incubated overnight at 4°C with anti-α-SMA (1:40, ab18147; Abcam), anti-uteroglobin (7G4E9, 1:100, ab50711; Abcam), anti-CD31/PECAM-1 (C31.7, NBP2–15188; Novus biological), anti-estrogen receptor alpha (sc-5002; Santa Cruz), and anti-progesterone receptor (sc-811; Santa Cruz) separately. Next, biotinylated goat anti-mouse IgG (BA 9200, 1:300; Vector laboratories), biotin-streptavidin HRP complex, and DAB chromogen (SK-415, ImmPACK DAB substrate kit; Vector Laboratories) were used to develop the reaction. CD31-stained slides were used for blood vessel density evaluation. The number of CD31-positive stained blood vessels in the endometrium was counted from at least 3 randomly selected fields per section under a magnification of 200×. All images were analyzed in a blind experiment using Olympus cellSens dimension software (version 1.16).

Western blot analysis.

Western blot analyses were performed at 6 months after implantation to compare smooth muscle actin protein expression among experimental groups. Frozen uterine tissue samples (10 mg) were homogenized in Pierce RIPA Buffer (89901; ThermoFisher Scientific) and

protein supernatant was collected. Protein concentration was determined using Pierce BCA Assay (ThermoFisher Scientific) and in one series of experiments, equal concentrations of protein from all groups were loaded for protein quantification. Protein samples (70μg/lane) were separated on 12% sodium dodecyl sulfate (SDS)–PAGE gels, and electroblotted to 0.45μm polyvinylidene difluoride (PVDF) membrane (ThermoFisher Scientific). The membranes were blocked with 5% milk powder for 1 hour at RT. Primary antibodies anti β-actin (1:200, sc-47778; Abcam) and Anti-α-SMA (1:200, ab-7187; Abcam) were diluted in blocking solution and incubated with membranes for 1 hour at RT. Membranes were incubated with peroxide-conjugated bovine anti-goat secondary antibody (1:1000, sc-2378; Santa Cruz Biotechnology) and stained with enhanced chemiluminescent substrate (Pierce) and protein signals were visualized with a LAS-3000 imaging system (Fujifilm). Images were densitometrically scanned using Image J (National Institutes of Health, Bethesda, MD) and protein quantification was analyzed with GraphPad Prism 8.0 for Windows (GraphPad Software, San Diego, CA). All densitometric raw data values for α-SMA were normalized to β-actin from the same sample lanes. Thus, a ratio of the amount of α-SMA, relative to an internal calibration of β-actin, was calculated for each group.

In vivo reproductive study.

Rabbits were naturally mated with fertile New Zealand male rabbits six months after undergoing the scaffold implantation procedure. Mating occurred in a breeding cage and was confirmed by observing male mounting behavior and the presence of sperm in vaginal smears. The mating day was considered gestation day zero, and the presence of fetuses was confirmed on standard radiographs taken at day 29–30. Pregnant rabbits were scanned using a computed tomography (CT) system (Aquilion 32; Toshiba) with a three-dimensional (3-D) body image reconstruction system to determine the fetus' positions in relation to the titanium clips placed around the bioengineered cell-seeded constructs.

Rabbit delivery/Cesarean section.

On day 29–30 of gestation, rabbits were administered buprenorphine (0.03 mg/Kg intramuscular) for sedation, and general anesthesia was induced and maintained on a ventilator with inhaled isoflurane (2–5%) and oxygen. Following a midline laparotomy, the pregnant uterus was exposed and examined for number of fetuses in relation to the engrafted site and uterine location. The viability and body weights of the delivered offspring were assessed at birth. All animals were euthanized following surgical delivery, and gross morphopathological analysis of the offspring was conducted by an independent pathologist.

Statistical analysis.

All values are expressed as the mean ± standard deviation (SD). For comparison of continuous variables across multiple groups, one-way analysis of variance (ANOVA) was performed followed by the Tukey test. Non-parametric analogs were applied for ordinal categorical variables. Fisher's exact test was performed to compare pregnancy rates. Statistical analyses were conducted using the R computer software for Windows (version 3.3.2). A p-value less than 0.05 was considered statistically significant. Due to the exploratory nature of the study, no adjustment for multiplicity was applied.

Data availability.

The data that supports the findings of this study are available from the corresponding author, upon reasonable request.

Supplementary Material

Refer to Web version on PubMed Central for supplementary material.

Acknowledgements

This work was supported by grants from the National Institutes of Health (T32-EB014836-05) and the State of North Carolina. We would like to thank J. Kassis for editorial assistance, T. Wang, H. G. Huddlestone, and C. Bishop for their initial background contribution to the project, and S. Lankford, A.S. Dean, I.Vasutin, T.J.Cockerham, M. Seeds, and E.E. Whitaker for technical assistance.

References

1. Taylor E & Gomel V The uterus and fertility. Fertility and sterility 89, 1–16, doi:10.1016/j.fertnstert.2007.09.069 (2008). [PubMed: 18155200]
2. Chan YY et al. Reproductive outcomes in women with congenital uterine anomalies: a systematic review. Ultrasound in obstetrics & gynecology : the official journal of the International Society of Ultrasound in Obstetrics and Gynecology 38, 371–382, doi:10.1002/uog.10056 (2011).
3. Abrao MS, Muzii L & Marana R Anatomical causes of female infertility and their management. International journal of gynaecology and obstetrics: the official organ of the International Federation of Gynaecology and Obstetrics 123 Suppl 2, S18–24, doi:10.1016/j.ijgo.2013.09.008 (2013).
4. Centers for Disease Control and Prevention. 2015 Assisted Reproductive Technology National Summary Report, <https://http://www.cdc.gov/art/pdf/2015-report/ART-2015-National-Summary-Report.pdf> (2017).
5. Fageeh W, Raffa H, Jabbad H & Marzouki A Transplantation of the human uterus. International journal of gynaecology and obstetrics: the official organ of the International Federation of Gynaecology and Obstetrics 76, 245–251 (2002).
6. Ozkan O et al. Preliminary results of the first human uterus transplantation from a multiorgan donor. Fertility and sterility 99, 470–476, doi:10.1016/j.fertnstert.2012.09.035 (2013). [PubMed: 23084266]
7. Brannstrom M et al. The first clinical uterus transplantation trial: a six-month report. Fertility and sterility, doi:10.1016/j.fertnstert.2014.02.024 (2014).
8. Brannstrom M et al. Livebirth after uterus transplantation. Lancet 385, 607–616, doi:10.1016/s0140-6736(14)61728-1 (2015). [PubMed: 25301505]
9. Testa G et al. First live birth after uterus transplantation in the United States. American journal of transplantation : official journal of the American Society of Transplantation and the American Society of Transplant Surgeons 18, 1270–1274, doi:10.1111/ajt.14737 (2018).
10. Baptista PM & Atala A Regenerative medicine: the hurdles and hopes. Translational research : the journal of laboratory and clinical medicine 163, 255–258, doi:10.1016/j.trsl.2014.01.008 (2014). [PubMed: 24524876]
11. Atala A, Bauer SB, Soker S, Yoo JJ & Retik AB Tissue-engineered autologous bladders for patients needing cystoplasty. Lancet 367, 1241–1246, doi:10.1016/S0140-6736(06)68438-9 (2006). [PubMed: 16631879]
12. L'Heureux N, McAllister TN & de la Fuente LM Tissue-engineered blood vessel for adult arterial revascularization. The New England journal of medicine 357, 1451–1453, doi:10.1056/NEJMc071536 (2007). [PubMed: 17914054]
13. Olausson M et al. Transplantation of an allogeneic vein bioengineered with autologous stem cells: a proof-of-concept study. Lancet 380, 230–237, doi:10.1016/s0140-6736(12)60633-3 (2012). [PubMed: 22704550]

14. Raya-Rivera A et al. Tissue-engineered autologous urethras for patients who need reconstruction: an observational study. Lancet 377, 1175–1182, doi:10.1016/s0140-6736(10)62354-9 (2011). [PubMed: 21388673]
15. Raya-Rivera AM et al. Tissue-engineered autologous vaginal organs in patients: a pilot cohort study. Lancet 384, 329–336, doi:10.1016/s0140-6736(14)60542-0 (2014). [PubMed: 24726478]
16. Campo H, Cervello I & Simon C Bioengineering the Uterus: An Overview of Recent Advances and Future Perspectives in Reproductive Medicine. Annals of biomedical engineering 45, 1710–1717, doi:10.1007/s10439-016-1783-3 (2017). [PubMed: 28028711]
17. Hellstrom M, Bandstein S & Brannstrom M Uterine Tissue Engineering and the Future of Uterus Transplantation. Annals of biomedical engineering 45, 1718–1730, doi:10.1007/s10439-016-1776-2 (2017). [PubMed: 27995397]
18. Ansari AH, Gould K & Turner RJ Segmental uterine horn replacement in rabbit using umbilical vein. Obstetrics and gynecology 60, 733–737 (1982). [PubMed: 7145278]
19. Taveau JW et al. Regeneration of uterine horn using porcine small intestinal submucosa grafts in rabbits. Journal of investigative surgery : the official journal of the Academy of Surgical Research 17, 81–92, doi:10.1080/08941930490422456 (2004). [PubMed: 15204714]
20. De Filippo RE, Yoo JJ & Atala A Urethral replacement using cell seeded tubularized collagen matrices. The Journal of urology 168, 1789–1792; discussion 1792–1783, doi:10.1097/01.ju.0000027662.69103.72 (2002). [PubMed: 12352360]
21. Dorin RP, Pohl HG, De Filippo RE, Yoo JJ & Atala A Tubularized urethral replacement with unseeded matrices: what is the maximum distance for normal tissue regeneration? World journal of urology 26, 323–326, doi:10.1007/s00345-008-0316-6 (2008). [PubMed: 18682960]
22. Fischer B, Chavatte-Palmer P, Viebahn C, Navarrete Santos A & Duranthon V Rabbit as a reproductive model for human health. Reproduction (Cambridge, England) 144, 1–10, doi:10.1530/rep-12-0091 (2012).
23. Atala A et al. Formation of urothelial structures in vivo from dissociated cells attached to biodegradable polymer scaffolds in vitro. The Journal of urology 148, 658–662 (1992). [PubMed: 1322466]
24. Oberpenning F, Meng J, Yoo JJ & Atala A De novo reconstitution of a functional mammalian urinary bladder by tissue engineering. Nature biotechnology 17, 149–155, doi:10.1038/6146 (1999).
25. De Filippo RE, Yoo JJ & Atala A Engineering of vaginal tissue in vivo. Tissue Eng. 9, 301–306, doi:10.1089/107632703764664765 (2003). [PubMed: 12740092]
26. Chen KL, Eberli D, Yoo JJ & Atala A Bioengineered corporal tissue for structural and functional restoration of the penis. Proceedings of the National Academy of Sciences of the United States of America 107, 3346–3350, doi:10.1073/pnas.0909367106 (2010). [PubMed: 19915140]
27. Atala A Engineering tissues, organs and cells. Journal of tissue engineering and regenerative medicine 1, 83–96, doi:10.1002/term.18 (2007). [PubMed: 18038397]
28. Park KR et al. CD9 is expressed on human endometrial epithelial cells in association with integrins alpha(6), alpha(3) and beta(1). Molecular human reproduction 6, 252–257, doi:10.1093/molehr/6.3.252 (2000). [PubMed: 10694273]
29. Cervello I et al. Reconstruction of endometrium from human endometrial side population cell lines. PloS one 6, e21221, doi:10.1371/journal.pone.0021221 (2011). [PubMed: 21712999]
30. Mosher AA et al. Development and validation of primary human myometrial cell culture models to study pregnancy and labour. BMC Pregnancy Childbirth 13 Suppl 1, S7, doi:10.1186/1471-2393-13-s1-s7 (2013). [PubMed: 23445904]
31. Wooding FB,G Comparative placentation : structures, functions, and evolution. 185–231 (Springer, 2008).
32. Jonkman MF, Kauer FM, Nieuwenhuis P & Molenaar I Segmental uterine horn replacement in the rat using a biodegradable microporous synthetic tube. Artificial organs 10, 475–480 (1986). [PubMed: 3800704]
33. Santoso EG et al. Application of Detergents or High Hydrostatic Pressure as Decellularization Processes in Uterine Tissues and Their Subsequent Effects on In Vivo Uterine Regeneration in Murine Models. PloS one 9, doi:Artn E103201

34. Campbell GR et al. The peritoneal cavity as a bioreactor for tissue engineering visceral organs: bladder, uterus and vas deferens. Journal of tissue engineering and regenerative medicine 2, 50–60, doi:10.1002/term.66 (2008). 10.1371/Journal.Pone.0103201 (2014). [PubMed: 18361481]

35. Li X et al. Regeneration of uterine horns in rats by collagen scaffolds loaded with collagen-binding human basic fibroblast growth factor. Biomaterials 32, 8172–8181, doi:10.1016/j.biomaterials.2011.07.050 (2011). [PubMed: 21821282]

36. Ding L et al. Transplantation of bone marrow mesenchymal stem cells on collagen scaffolds for the functional regeneration of injured rat uterus. Biomaterials 35, 4888–4900, doi:10.1016/j.biomaterials.2014.02.046 (2014). [PubMed: 24680661]

37. Song T et al. Regeneration of uterine horns in rats using collagen scaffolds loaded with human embryonic stem cell-derived endometrium-like cells. Tissue engineering. Part A 21, 353–361, doi:10.1089/ten.TEA.2014.0052 (2015). [PubMed: 25097004]

38. Miyazaki K & Maruyama T Partial regeneration and reconstruction of the rat uterus through recellularization of a decellularized uterine matrix. Biomaterials 35, 8791–8800, doi:10.1016/j.biomaterials.2014.06.052 (2014). [PubMed: 25043501]

39. Hellstrom M et al. Bioengineered uterine tissue supports pregnancy in a rat model. Fertility and sterility, doi:10.1016/j.fertnstert.2016.03.048 (2016).

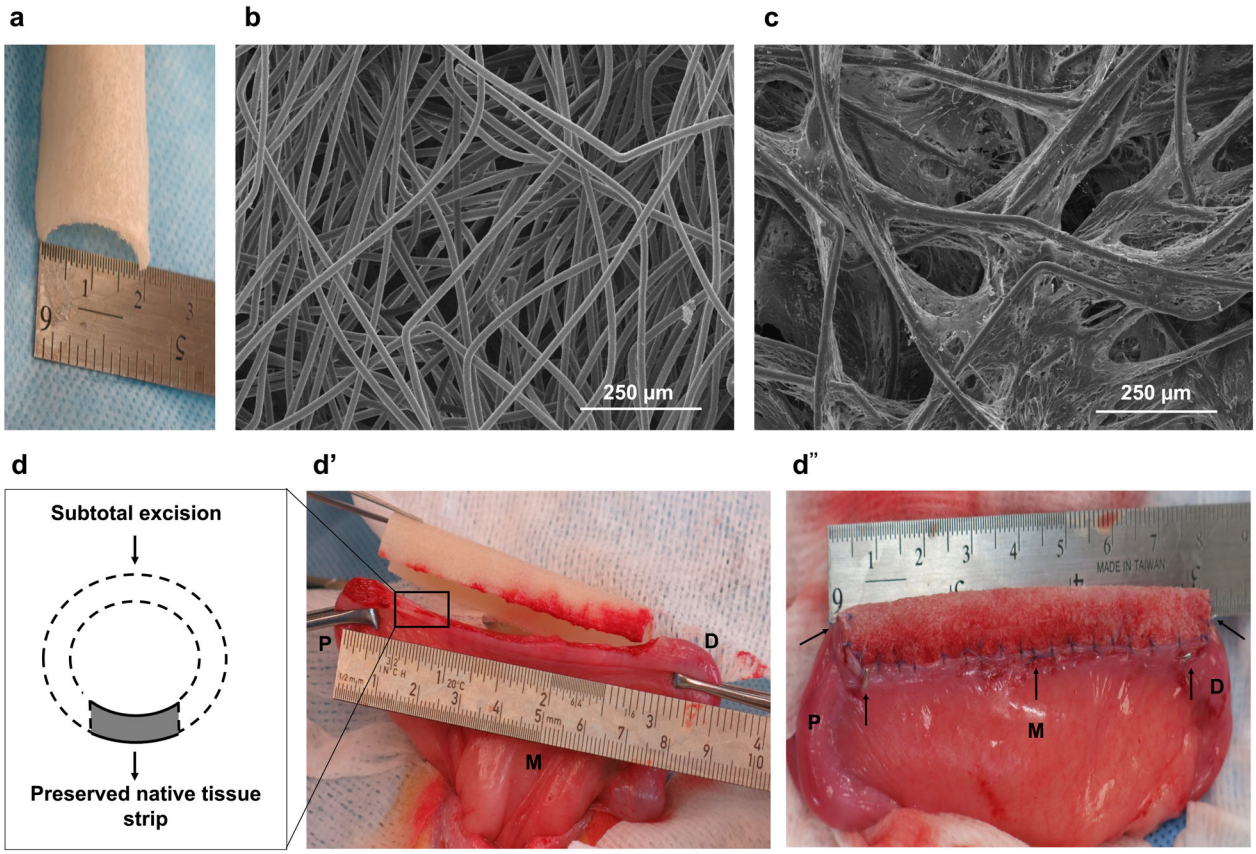

Figure 1.

Construct fabrication and in vivo implantation. (**a**) Gross image of the synthetic polymer scaffold; (**b**) Scanning electron microscopy (SEM) image showing the porous microstructure of the scaffold. (**c**) Representative SEM image of a cell-seeded construct prior to implantation. Experiments were repeated independently three times with similar results. (**d**) Schematic drawing of the subtotal uterine excision and scaffold implantation procedures; (**e**) surgical excision of one uterine horn and scaffold implantation; (**f**) the engrafted uterine horn. Black arrows indicate tag sutures and titanium clips inserted at the anastomosis; P = proximal native tissue retained at the cervical end; M = mesometrium (mesentery to the uterus); D = distal native tissue retained at the tubal end.

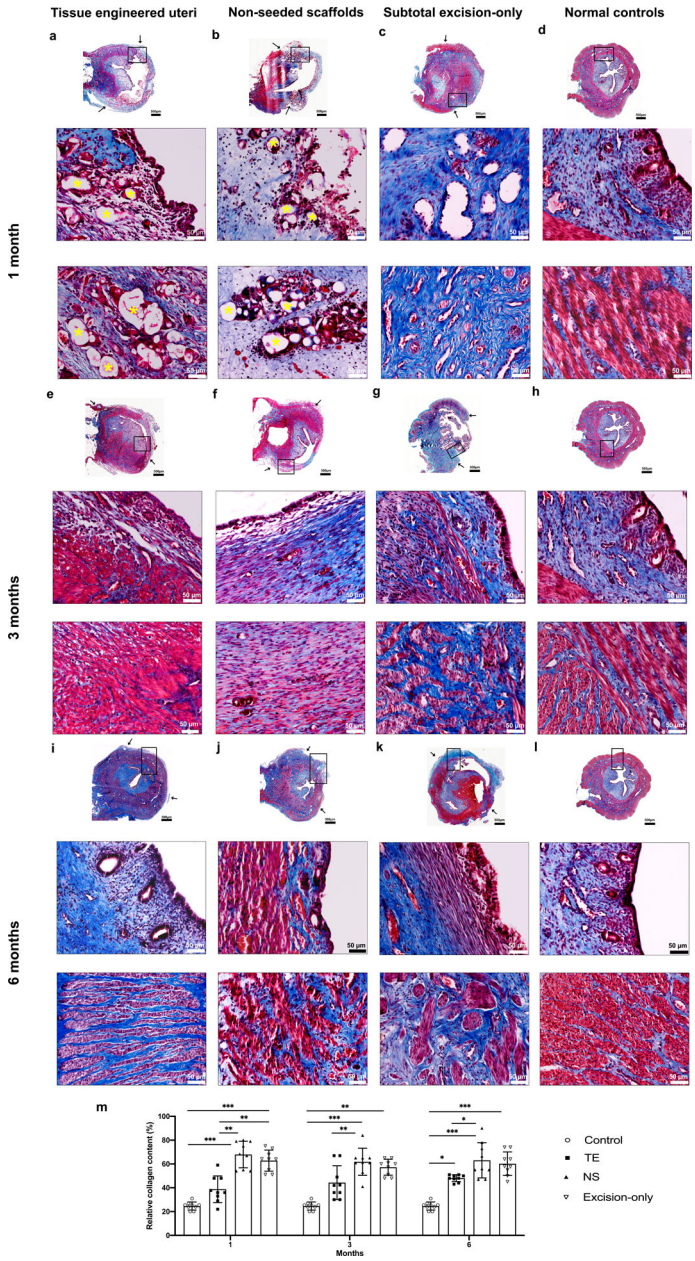

Figure 2.

Histological analysis of Masson's trichrome (MT) stained cross-sections of reconstructed uterine segments retrieved at 1 (**a - d**) 3 (**e - h**), and 6 (**i - l**) months post-surgery. (**a**-**b**) At one-month post-implantation, partially degraded polymer material (yellow asterisk) was observed in the endometrium (**a middle, b middle**) and myometrium (**a middle- b bottom**) regions in the tissue engineered uteri and non-seeded scaffold groups. The subtotal excision-only group showed abundant granulomatous tissue accompanied by luminal strictures (**c middle and bottom**). (**e, f**) At three months, the polymer material was completely resorbed. Distinct lining endometrium (**e middle**) and myometrium structure (**e bottom**) developed in the tissue engineered uteri group, whereas the non-seeded group had sparse tissue ingrowth (**f middle –f bottom**), and the subtotal excision-only group had marked defects in the

uterine wall (**g**). (**i - l**) Six months after surgery, the engineered seeded constructs showed organized tissue structures with native-like endometrium (**I middle**) and myometrium layers (**I bottom**), while the non-seeded scaffolds formed a thin uterine wall (**j**), and the subtotal excision-only controls showed scar formation (**k**). (**m**) Statistical analysis of the relative collagen content in MT stained slides (under a magnification of 100×) demonstrated that the non-seeded scaffold group formed the most collagen tissue overall. MT staining: blue, collagen/connective tissue; red, smooth muscle. Black arrows indicate the interface between the native uterine tissue and surgical area. Data shown are representative images from n=3 animals per time point in each group; experiments were repeated independently three times with similar results. One-tailed one-way ANOVA was performed followed by the Tukey test. Error bars, mean ± SD. * $P < 0.05$, ** $P < 0.01$, *** $P < 0.001$. Scale bars 500 μm; 50 μm.

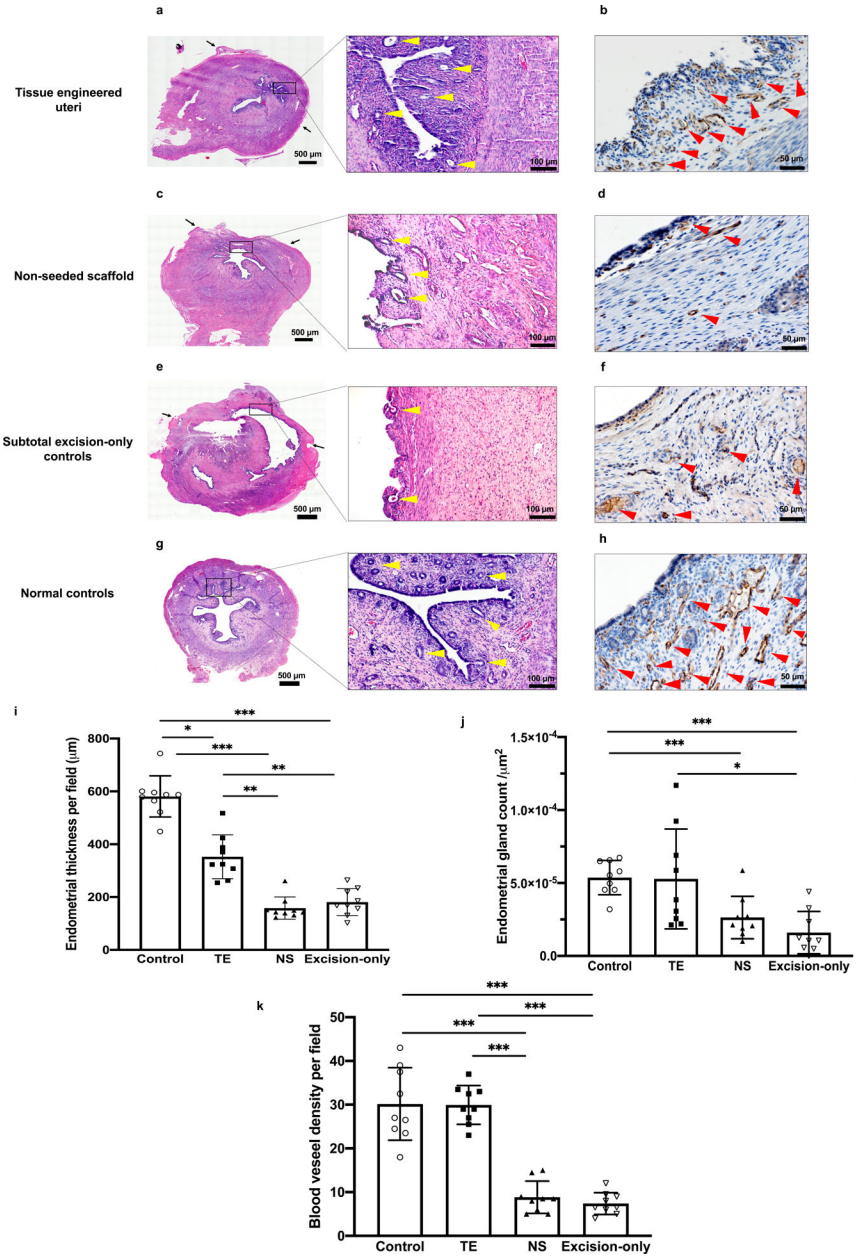

Figure 3.

Histomorphological analysis of the uterine mucosa at 6 months post implantation. (**a, c, e, g**) Hematoxylin-eosin (H&E) cross-sections of uterine horns. (**b, d, f, h**) Immunostaining for CD31 indicates positive endothelial cells in the capillaries and lining of mature blood vessels. (**i**) Analysis of the average endometrial thickness measured at the points of greatest perpendicular depth under a magnification of 100× showed that the tissue engineered uteri group formed thicker inner layer than the non-seeded scaffold group and subtotal excision-only controls. (**j**) Quantitative analysis of the average number of endometrial glands per field using a 20× objective showed that the endometrial gland density was comparable between the tissue engineered uteri group and normal controls. (**k**) Quantitative analysis of the average number of microvessels per field under a magnification of 200× showed greater

endometrium neovascularization in tissue engineered uteri group than the non-seeded group and subtotal excision-only group. Black arrows indicate the interface between the native uterine tissue and engrafted site; Scale bar 500μm; 100 μm; 50 μm. Yellow arrowheads indicate endometrial glands; red arrowheads indicate blood vessels. Data shown are representative images from n = 3 animals per group; experiments were repeated independently three times with similar results. One-tailed one-way ANOVA was performed followed by the Tukey test. Error bars, mean ± SD. * $P < 0.05$, ** $P < 0.01$, *** $P < 0.001$.

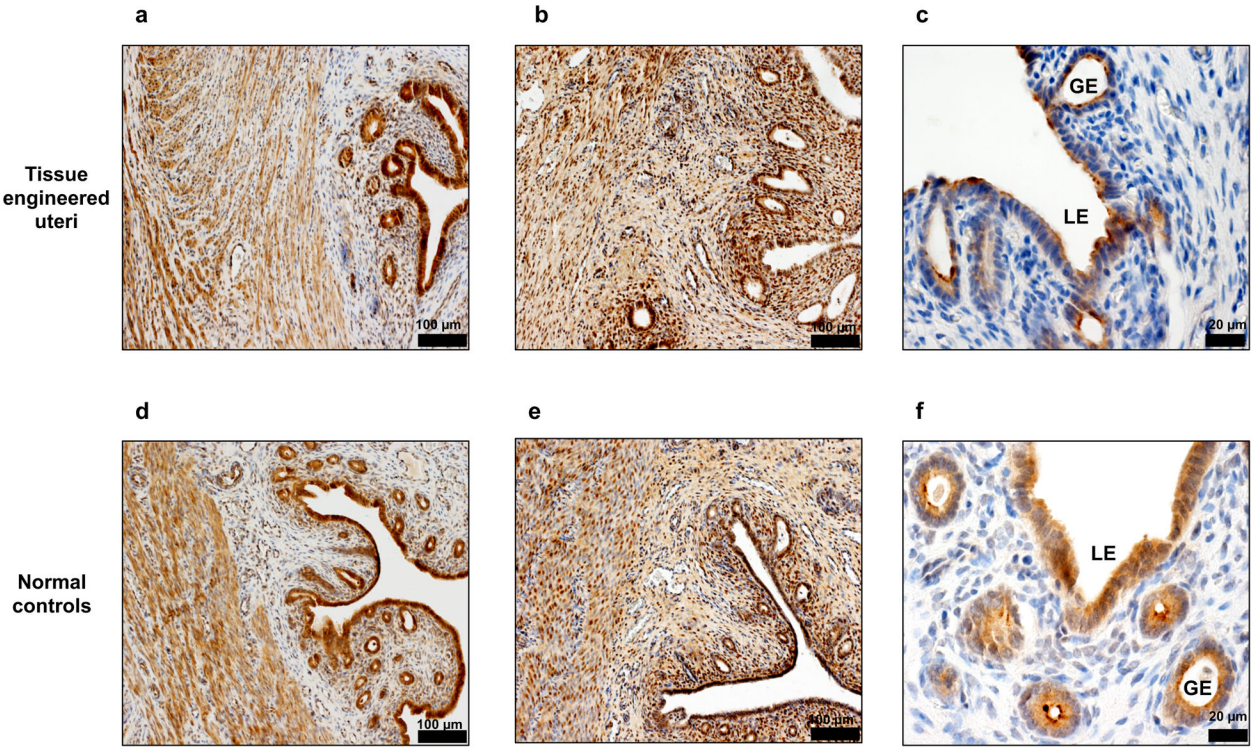

Figure 4.

Immunohistochemical staining of functional markers in the tissue engineered uteri at 6 months post implantation. (**a,d**) Estrogen receptor alpha positive cells in the endometrium and myometrium layers. Scale bar: 100 μm (**b,e**) Progesterone receptor expression in epithelial and stromal cells. Scale bar: 100 μm (**c,f**) Detection of uteroglobin expression showed the presence of secretory glands structure in the engineered uteri. Data shown are representative images from n = 3 animals; experiments were repeated independently three times with similar results. Scale bar: 20 μm. LE: luminal epithelium. GE: glandular epithelium.

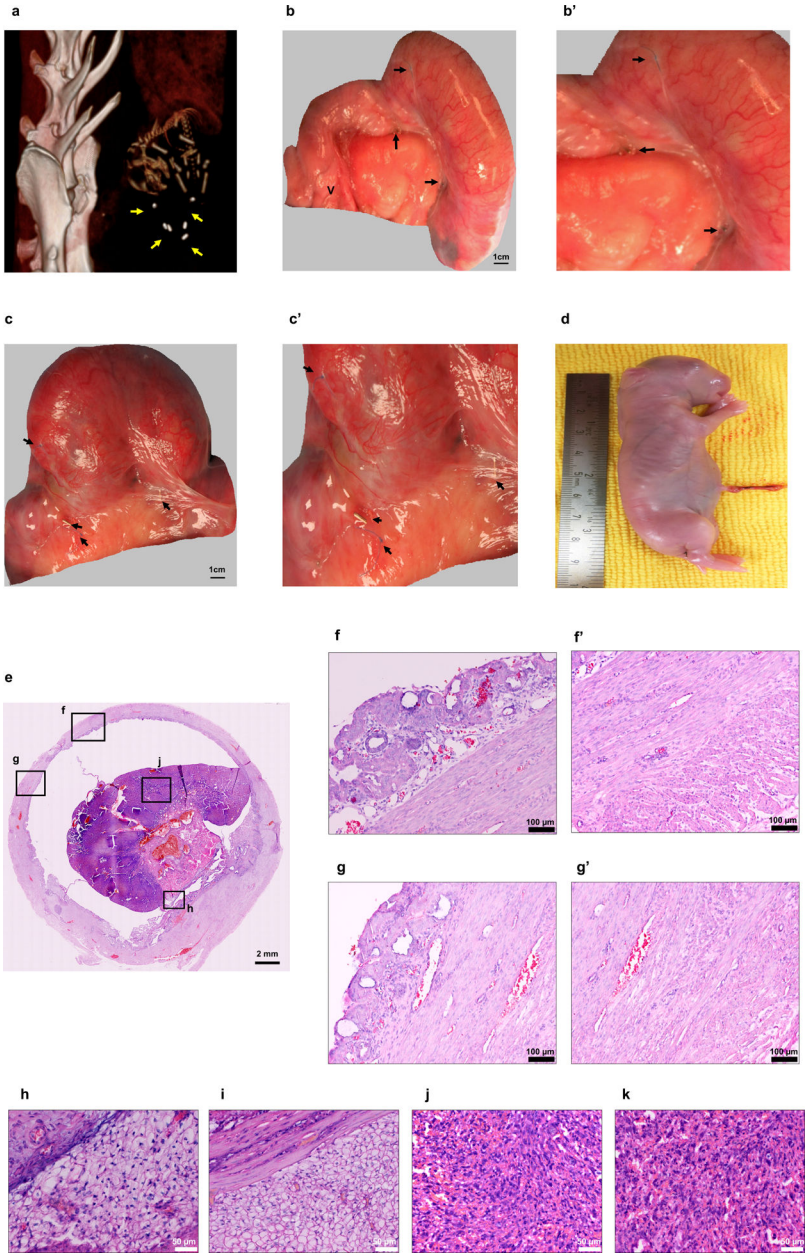

Figure 5.

Fetal development site identification at day 29–30 post mating in a single-horn pregnant uterus. (**a**) Computed tomography image of a fetus within the tissue engineered uterus, demarcated by the titanium clips. (**b-c**) Pregnancies in the tissue engineered uteri group at birth. Scale bar: 1 cm. (**b'-c'**) Titanium clips and marking sutures indicated that fetal development occurred within the bioengineered segment. (**d**) Gross appearance of a newborn from a tissue engineered uterus. (**e**) H&E stained cross-section of the pregnant bioengineered uterus. Scale bar: 2 mm (**f, g**) Micrographs of the pregnant engineered uterine wall revealed structural integrity of the endometrial and myometrial layers (**f', g'**). Scale bar: 100 µm (**h, i**) Decidua. (**h**) Decidua zone in the tissue engineered uteri group; (**i**) decidua zone in normal controls. (**j, k**) Rabbit placenta. (**j**) Labyrinth zone in the tissue engineered

uteri group; (**k**) labyrinth zone in normal controls. Scale bar: 50 μm. Yellow arrows indicate titanium clips; black arrows indicate the titanium clips and non-absorbable sutures at the margins of the engrafted tissue. Data shown are representative images from n = 4 animals; experiments were repeated independently three times with similar results. V: vagina.

Table 1.

Reproductive outcomes in experimental rabbits.

Outcomes	Tissue engineered uteri group (n=14)		Non-seeded scaffold group (n=14)		Subtotal excision-only controls (n=7)	Normal controls (n=7)	p-value
Uterine Segment	**Engineered**	**Native**	**Scaffold only**	**Native**	**Native**	**Native**	
Pregnancy rate	4/14, 28.5%[g]	6/14, 42.8%[g]	0/14, 0%	7/14, 50%	1/7, 14.3%	7/7,100%[e,f]	< 0.01[b]
Term delivery	3/4, 75%	6/6, 100%	0/14, 0%	5/7, 71.4%	0/1, 0%	7/7, 100%	0.093[b]
Average litter per pregnancy[a]	1	1.4 ± 0.8	N/A	1	1	3.9 ± 1[h,f]	≤0.001[c]
Offspring average body weight at birth (g)	46.7 ± 9.5	42.6 ± 9	N/A	44 ± 11	N/A	45.5 ± 5.3	0.994[d]

Engineered refers to the site receiving a cell-seeded bioengineered construct; Native corresponds to either the remaining normal uterine tissue proximal to the implantation site or the tissue in the normal controls; Scaffold only refers to the site receiving the scaffold alone, without the cells.

[a] Average litter per pregnancy: the average number of fetuses in a single-horn pregnant uterus.

[b] Fisher exact test,

[c] Kruskal-Wallis test and

[d] One-tailed one-way ANOVA test; critical level of significance, $p < 0.05$.

[e] $p < 0.05$, Normal controls versus subtotal excision-only controls.

[f] $p < 0.05$, Normal controls versus non-seeded scaffolds group.

[g] $p < 0.05$, Tissue engineered uteri group versus subtotal excision-only controls.

[h] $p < 0.05$, Normal controls versus tissue engineered uteri group.

Data are presented as mean ± SD.